PHYSICAL REVIEW

LETTERS

VOLUME 63 9 OCTOBER 1989 NUMBER 15

Results of a New Test of Local Lorentz Invariance: A Search for Mass Anisotropy in ^{21}Ne

T. E. Chupp, R. J. Hoare, R. A. Loveman, E. R. Oteiza, J. M. Richardson, and M. E. Wagshul
The Physics Laboratories, Harvard University, Cambridge, Massachusetts 02138

A. K. Thompson
Massachusetts Institute of Technology, Cambridge Massachusetts 02139
(Received 23 March 1989; revised manuscript received 10 July 1989)

We test Lorentz invariance by searching for a time-dependent quadrupole splitting of Zeeman levels in ^{21}Ne. A component at twice the Earth's sidereal frequency would suggest a preferred direction which affects the local physics of the nucleus. The technique employs polarized ^{21}Ne and ^{3}He gases produced by spin exchange with laser optically pumped Rb. Both species are contained in the same glass cell; ^{3}He provides magnetometry and a monitor of systematic effects. Our data produce an upper limit (1σ confidence level) of 2×10^{-21} eV (0.45×10^{-6} Hz) on the Lorentz-invariance–violating contribution to the binding energy. This result is comparable to that of the most precise previous experiment.

PACS numbers: 04.80.+z, 07.58.+g, 32.60.+i

Local Lorentz invariance (LLI) along with the postulates of local position invariance and the weak equivalence principle form the Einstein equivalence principle, the basis of all single-metric gravitational theories.[1,2] LLI requires that the local, nongravitational physics of a bound system of particles be independent of its velocity and orientation relative to any preferred frame, for example, the rest frame of the Universe.[3] If LLI were violated and such a frame existed, the energy levels of a bound system such as a nucleus could be shifted in a way that correlates the motion of the bound particles in each state with the preferred direction. Such a shift would lead to an orientation-dependent binding energy, i.e., an anisotropy of inertial mass. The lowest-order, nonvanishing effect of this sort would lead to a quadrupole splitting of the nuclear Zeeman levels since a dipole coupling of the preferred direction to the position or velocity of the particles in the bound system would have vanishing expectation value. (We note, however, that there may exist the coupling of the dipole moment of the nucleus to a cosmic field such as that of relic neutrinos or that postulated to be produced by axions.[4]) The first tests of this sort, known as Hughes-Drever experiments, were performed by Hughes, Robinson, and Beltran-Lopez[5] and by Drever,[6] with modern, much more precise measurements by Prestage *et al.*[7] and by Lamoreaux *et al.*[8] The most precise previous measurement[8] set a 2σ upper limit of 0.5×10^{-6} Hz on any such LLI-violating quadrupole splitting, which is 10^{-28} of the binding energy per nucleon. Our work provides a comparable limit.

We have chosen ^{21}Ne with nuclear spin $I_{21}=\frac{3}{2}$ to perform such a test. A mixture of ^{21}Ne and ^{3}He (nuclear spin $I_3=\frac{1}{2}$) can be simultaneously polarized by spin exchange with laser optically pumped Rb vapor.[9–11] The energy differences among the Zeeman levels of each species are measured by observing the free precession of the spins. The ^{21}Ne would be sensitive to the preferred direction, leading to a shift of the $m=\pm\frac{3}{2}$ levels different from that of the $m=\pm\frac{1}{2}$ levels. The ^{3}He is not sensitive to the quadrupole splitting and has the multiple role of a magnetometer and a monitor of systematic effects.

The apparatus is shown in Fig. 1. The laser system is a krypton-ion laser pumping LD-700 dye in a standing-wave, multimode dye laser. A 500-mW diode-laser array has also been used; however, the results presented here are based on runs with the dye-laser system. The laser light optically pumps the Rb-$D1$ resonance line which is pressure broadened so that the absorption linewidth is about 25 GHz. The Rb is contained in a nearly spherical alumino-silicate glass cell with about 400 Torr (at 300 K) each of ^{21}Ne and ^{3}He and 60 Torr of N_2 to

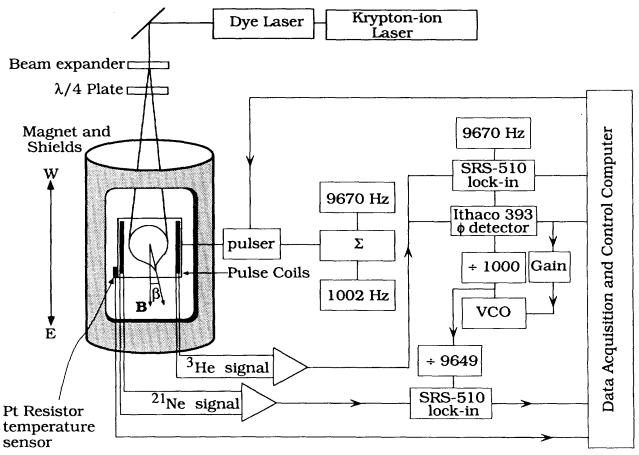

FIG. 1. A schematic diagram of the apparatus as described in the text. The magnet consists of a pair of solenoids of opposite polarity within a three-layer Mumetal magnetic shield. The axes of the solenoids, the pulse coils, and the pair of pickup coils are orthogonal.

suppress radiation trapping effects. The cell is contained in an oven heated by flowing hot air. NMR pulse and pickup coils and static-field trim coils are mounted on the oven. The cell's spherical symmetry is most strongly broken by the "pull-off" seal as illustrated. This provides for an axis of cylindrical symmetry of the cell which is oriented relative to the static magnetic field (**B**) at an angle β. A quadrupole splitting of $\approx 240 \times 10^{-6}$ Hz is induced by coupling of the nuclear electric quadrupole moment to electric field gradients at the cell wall which do not average to zero due to the asymmetry of the cell. This induced splitting is proportional to $P_2(\cos\beta)$ and is temperature dependent as described below.[12] We have set $\beta \approx 0$ in order to have minimum sensitivity to changes in β. The entire assembly is placed within a magnet constructed of two coaxial solenoids with opposite polarity and current densities arranged to cancel the distant magnetic dipole moment. This allows effective use of a three-layer Mumetal magnetic shield which is neither saturated nor magnetized by the 3-G field within the solenoids. The magnetic field gradients in the region of the cell are adjusted to be less than 10^{-5} G/cm. The magnetic field can be stabilized with a diode-laser–pumped Rb magnetometer located near the oven assembly. The actual magnetic field variations are less than 10^{-6} G. As described below, ^{3}He magnetometry is employed in signal processing to compensate for these variations to the level of 10^{-10} G.[11] The axis of the magnetic field is oriented within 2° of the east-west direction so that, as the Earth rotates, the orientation of the apparatus changes with respect to all directions except that of the Earth's axis.

The atoms are initially polarized along (or against) **B**. An individual free-precession measurement is initiated by a 50-ms pulse of time-varying magnetic field with components at the Larmor frequencies of both the ^{21}Ne and ^{3}He. The atoms' spins are tilted by about 30° relative to **B** producing transverse and longitudinal components of the magnetization. The relaxation times for the components of magnetization are T_1 (longitudinal component) 1.8 h for ^{21}Ne and 10 h for ^{3}He, and T_2 (transverse component) 1.8 h for ^{21}Ne and 0.2–1.1 h for ^{3}He. For ^{21}Ne, both relaxation times are dominated by atom-wall interactions. For ^{3}He, the wall interaction dominates T_1 and magnetic field inhomogeneity dominates T_2. The laser is blocked during measurement of the atoms' free-precession frequency spectra so that the Rb is not optically pumped.

The spins precess freely about **B** at frequencies near 1000 Hz for ^{21}Ne and 9650 Hz for ^{3}He and the changing magnetization induces voltages in two pickup coils, one tuned to 4 kHz (for the ^{21}Ne) and the other to 20 kHz (for the ^{3}He). These frequencies were chosen so that the precession frequencies were far below resonance for both tuned circuits in order that the nonlinear effects of atom-cavity coupling would be minimized and the response to the induced voltage would be unity. The signal from each coil is buffered, amplified, and then processed as described below. The typical signal size for the ^{21}Ne is 1 μV and for the ^{3}He is 10 μV while the total noise density due to Johnson noise from the pickup coils and amplifier noise is 4 nV/$\sqrt{\text{Hz}}$.

The ^{3}He signals are fed to a phase-locked loop (PLL) which locks a voltage-controlled oscillator (VCO) to 1000 times the precession frequency. The phase detector is an Ithaco 393 two-phase lock-in amplifier. The VCO frequency is divided by 9649 to provide a reference frequency that is about $\frac{1}{60}$ Hz different from the ^{21}Ne precession frequency. This reference frequency is beat against the signals from the ^{21}Ne channel with the linear sine-wave mixers in the Stanford Research Systems 151 lock-in amplifier. The low-pass filter is set to 3 or 10 s. The signals from the ^{3}He channel are beat against a fixed reference frequency derived from a 10-MHz oven-stabilized quartz clock. The beat signals are read by a 12-bit analog-to-digital converter (ADC) interfaced to the data acquisition and control computer. In addition, the phase-locked-loop error signal and temperature at three positions on the oven are read by the ADC. All signals are converted at 1-s intervals timed by the same 10-MHz clock. In setup runs, we have monitored the ambient magnetic field in the room and the magnet current but these quantities are less sensitive to systematic effects than the other monitors we have developed.

A single free-precession measurement lasts from 45 min to 1 h. The useful data exclude an initial period of 20 to 60 s during which pulse-related transients decay and the times after the ^{3}He signal has decayed enough to effect the PLL. In Fig. 2(a) we show the time-domain signals from the ^{21}Ne, $S_{21}(t)$, for a typical run. The shape of the time-domain signal is the result of beats due

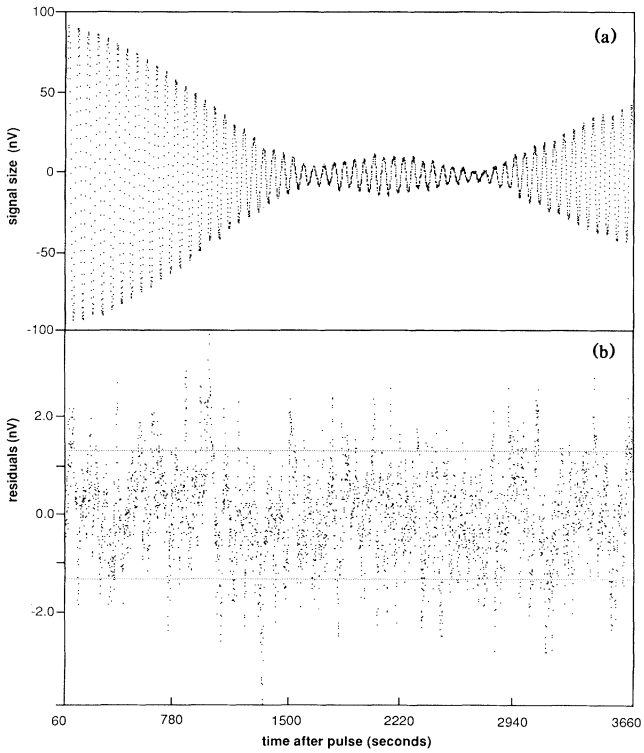

FIG. 2. The data from a single run of duration 3660 s. The data for the first 60 s, after which transients due to the NMR pulse have decayed, are discarded. (a) The data as measured at 1-s intervals. (b) The residuals for the best fit with the ten-parameter model described in the text. The error of ± 1.3 nV is indicated by the dotted lines.

to the interference of the three frequencies corresponding to the splittings between pairs of Zeeman levels with $|\Delta m_F| = 1$. Relaxation of the signal at the rate $1/T_2$ is also evident in Fig. 2(a). In the time domain $S_{21}(t)$ can be represented as

$$S_{21}(t) = \kappa \left\{ \sum_{i=1}^{3} C_i \cos[\omega_i t + \phi_i] \right\} e^{-t/T_2}, \quad (1)$$

where κ provides for the calibration of signal size,

$$C_i \cos\phi_i = [I(I+1) - m(m-1)]^{1/2} \mathrm{Re}(A_m^* A_{m-1})$$

at $t = 0$, and A_m is the amplitude to find a ^{21}Ne atom in the state $|m\rangle$. The frequencies ω_i are

$$\omega_1 = \omega_{3/2,1/2} = 2\pi(D + Q + \tfrac{13}{12} O),$$
$$\omega_2 = \omega_{1/2,-1/2} = 2\pi(D + \tfrac{1}{12} O), \quad (2)$$
$$\omega_3 = \omega_{-1/2,-3/2} = 2\pi(D - Q + \tfrac{13}{12} O).$$

D, Q, and O are, respectively, dipole, quadrupole, and octupole splittings of the Zeeman levels measured in Hz (cycles per second).

We have fitted the time-domain data for each run by χ^2 minimization with a model based on Eq. (1) with a constant term added to account for offsets in the electronics. The noise at the ^{21}Ne precession frequency was directly measured in a run with ^{3}He magnetometry but without ^{21}Ne signals. This was used as the uncertainty for each time-domain reading. We have tested for an octupole splitting which would arise from the coupling of magnetic field gradients to the magnetic octupole moment of the nucleus. No statistically significant octupole coupling is evident as expected in the very uniform magnetic field, and O is set to zero in the model used to fit the data. The residuals for the fit to the data of Fig. 2(a) are shown in Fig. 2(b). The uncertainty for each time-domain reading (± 1.3 nV) is indicated by the pair of horizontal dotted lines. The χ^2 per degree of freedom is consistently less than or equal to 1.0. The uncertainty in the best fit value for Q is typically $(0.5\text{–}1.0)\times 10^{-6}$ Hz.

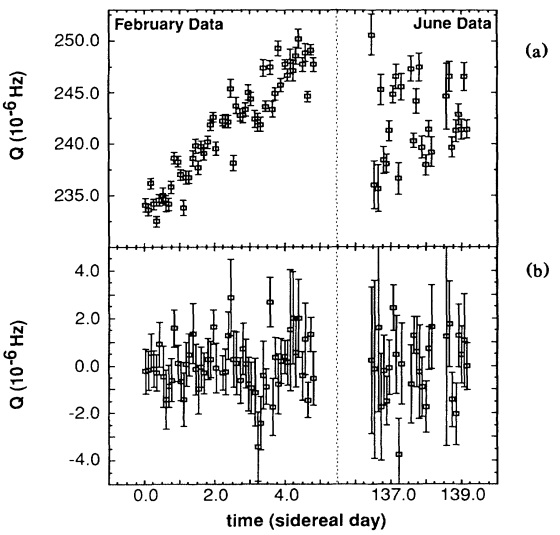

FIG. 3. The data for the two runs. (a) The raw data for $Q(t)$, the size of the quadrupole splitting in ^{21}Ne. (b) The residuals after the raw data are fitted for drifts linear and quadratic in time and for cell temperature variations. The error bars in (b) are adjusted to reflect the value of χ^2/N_{DF} for the first 5-day run.

In Fig. 3 we summarize the results for data taken 2–9 February 1989, for five days, and 25–29 June 1989, for three days. Time $t = 0$ was 19:30:00 Greenwich mean time on 9 February 1989. The time assigned to each run is its midpoint. Each run was started 2 h and 1 min later than the previous run to prevent synchronizing the data with hourly events. For each run the data are fitted with the model described in the previous paragraphs.

The raw data for each run are predominantly characterized by a linear drift in time and fluctuations due to the change of the cell wall temperature. We attribute the larger linear time dependence during the February run to a combination of gradual changes in the cell wall, mostly due to reaction of the Rb, and possible mechanical relaxation of the oven assembly and magnet resulting in change of the angle β. Changes in the cell wall tem-

perature are most accurately monitored with the wall relaxation rate (Γ_w). Wall relaxation results from the interaction of the magnetic and electric moments of the ^{21}Ne nucleus with fields at the wall during the time the atom is resident before "evaporating" from a van der Waals well at the wall. The total wall relaxation rate is proportional to the time spent at the wall, i.e., proportional to $e^{T_w/T}$, where kT_w is the effective well depth. Small changes in T are therefore proportional to Γ_w. One might worry that this temperature correction would hide a LLI-violating effect. This is not the case, for relaxation is due to the mixing of the Zeeman levels, not the shift of energies for which we are searching.

The data were separately analyzed for each run. We first remove the temperature correlation by fitting with a model with a constant term, terms linear and quadratic in time, and a term proportional to $1/T_2$ of ^{21}Ne. The error in Q for each measurement was adjusted to account for the uncertainty in the best-fit value of Γ_w. We have tried adding terms to the model linear in each of the oven temperature monitors and the signal size as well as products of these with no statistically significant improvements of the fit. We therefore conclude that any first- or second-order correlation with these quantities is negligible.

The residuals, shown in Fig. 3(b), are then used to search for a periodic component at $2\Omega_S$. The error bars for the February run are corrected by the square root of the χ^2 per degree of freedom ($\chi^2/N_{\rm DF}=85/53$). The $\chi^2/N_{\rm DF}$ for the June rune is 20/24. Two methods are applied to extract this component. In the first, the data are treated as a coherent sample. In the second, the data, modulo one sidereal day, are assigned to 21 bins of four measurements each with the weighted average for Q in each bin and the weighted average time used to produce a record in time. The best-fit value for the amplitude of the $2\Omega_S$ component is

$$\begin{aligned} Q_S &= (0.18\pm0.17)\times10^{-6}\ \text{Hz}\ \ \text{(method 1)}, \\ Q_S &= (0.15\pm0.19)\times10^{-6}\ \text{Hz}\ \ \text{(method 2)}. \end{aligned} \tag{3}$$

We also examined each run separately. Both contain a component at $2\Omega_S$ at the 2σ level. This is probably due to diurnal temperature fluctuations in the laboratory. These fluctuations are dominated by a one-day cycle which also has components near $2\Omega_S$ and $3\Omega_S$. The combination of the February and June runs tends to smooth the effects of these fluctuations because the phase difference between the sidereal day and solar day have advanced 120°, and the phase difference between 2Ω components is 240°.

A modern analysis of these experiments has been presented by Haugen and Will[13] in the context of a model in which the electromagnetic binding energy transforms under Lorentz boosts differently than inertial mass (the $TH\epsilon\mu$ model of Lightman and Lee[14]). Prestage *et al.*[7] use this model to show that for an angle α between the quantization axis and the preferred direction the local-Lorentz-invariance-violating contribution to the inertial mass of a nucleus is given by

$$\Delta m = \left(1-\frac{c^2}{c_0^2}\right) M_{\rm EM}\frac{Q}{6R^2}\frac{\mathbf{v}^2}{c_0^2}P_2(\cos(\alpha))\,. \tag{4}$$

Here Q/R^2 is the normalized quadrupole moment of the ^{21}Ne nucleus, $M_{\rm EM}=(Z-1)e^2/R$ is the electromagnetic potential energy for a proton, c and c_0 are the space-time connections (limiting velocities) for the two forms of mass-energy, and $\mathbf{v}$ is the velocity of the laboratory relative to the preferred frame taken to be $10^{-3}c$, the speed of the Earth's motion relative to the rest frame of the Universe. The quantity $1-c^2/c_0^2$ is a measure of the preferred-frame effects. Our results set limits $\Delta m<2\times10^{-21}$ eV (0.45×10^{-6} Hz) and $1-c^2/c_0^2<3\times10^{-21}$. The model of Eq. (4) is specific to the electromagnetic contribution to the binding energy of the nucleus. The Lorentz transformation properties of other forms of binding energy, specifically that due to the strong interaction, may lead to mass anisotropy. A rigorous analysis has not been undertaken but it is expected that tighter limits on $1-c^2/c_0^2$ would result.

The limits set by this measurement are a factor of 400 less than that reported by Prestage *et al.*[7] Lamoreaux *et al.* quote a 2σ limit of 0.5×10^{-6} Hz which is comparable to our 2σ limit of 0.7×10^{-6} Hz. We expect improved limits with the current setup by combining data taken at three-month intervals and for longer periods. The statistical precision for each measurement of Q can also be improved by effecting longer T_2 for the ^{3}He, perhaps by using the coupling between spins and the pickup coils that has been suppressed in these measurements.

We wish to acknowledge useful discussions in the early stages of this work with A. B. McDonald, J. Peebles, and R. Dicke as well as E. N. Fortson, S. Lamoreaux, B. Heckle, W. Happer, and M. P. Haugen. Kamakshi Rao and J. Hobson assisted in the reduction of much of the data. This work was supported by a National Bureau of Standards Precision Measurement grant, the National Science Foundation, and the Research Corporation. T.E.C. also acknowledges support of the Alfred P. Sloan Foundation.

[1]K. S. Thorne, D. L. Lee, and A. P. Lightman, Phys. Rev. D **7**, 3563 (1973).

[2]C. M. Will, *Theory and Experiment in Gravitational Physics* (Cambridge Univ. Press, New York, 1981).

[3]P. Lubin, T. Villela, G. Epstein, and G. Smoot, Astrophys. J. **298**, L1 (1985).

[4]L. Abbott and P. Sekivie, Phys. Lett. **120B**, 133 (1983).

[5]V. Hughes, H. G. Robinson, and V. Beltran-Lopez, Phys. Rev. Lett. **4**, 342 (1960).

[6]R. P. W. Drever, Philos. Mag. **6**, 683 (1961).

[7]J. D. Prestage, J. J. Bollinger, W. M. Itano, and D. J.

Wineland, Phys. Rev. Lett. **54**, 2387 (1985).

[8]S. K. Lamoreaux, J. P. Jacobs, B. R. Heckel, F. J. Raab, and E. N. Fortson, Phys. Rev. A **39**, 1082 (1989).

[9]T. E. Chupp and K. P. Coulter, Phys. Rev. Lett. **55**, 1074 (1985).

[10]T. E. Chupp, M. E. Wagshul, K. P. Coulter, A. B. McDonald, and W. Happer, Phys. Rev. C **36**, 2244 (1987).

[11]T. E. Chupp, E. R. Oteiza, J. M. Richardson, and T. R. White, Phys. Rev. A **38**, 3998 (1988).

[12]Z. Wu, S. Schaefer, G. D. Cates, and W. Happer, Phys. Rev. A **37**, 1161 (1988).

[13]M. P. Haugen, Ann. Phys. (N.Y.) **118**, 156 (1979); M. P. Haugen and C. M. Will, Phys. Today **40**, No. 5, 69 (1987).

[14]A. P. Lightman and D. L. Lee, Phys. Rev. D **8**, 364 (1973).

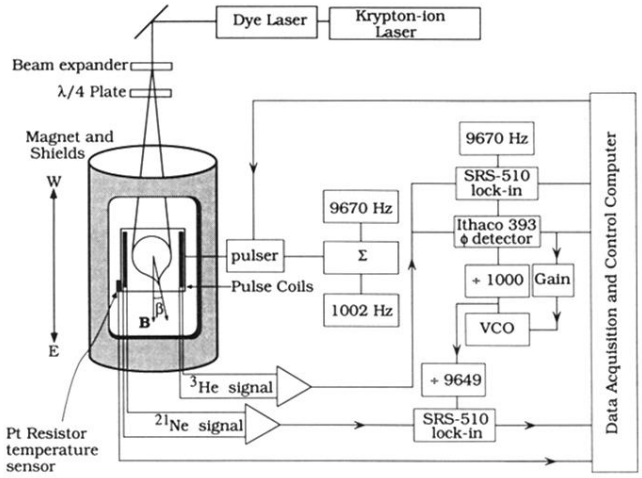

FIG. 1. A schematic diagram of the apparatus as described in the text. The magnet consists of a pair of solenoids of opposite polarity within a three-layer Mumetal magnetic shield. The axes of the solenoids, the pulse coils, and the pair of pick-up coils are orthogonal.